J. Eur. Opt. Society-Rapid Publ. 2026, **22**, 12

https://doi.org/10.1051/jeos/2025053
Available online at: https://jeos.edpsciences.org

Journal of the European Optical Society-Rapid Publications

RESEARCH ARTICLE OPEN ACCESS

Structural colour and photonic mechanisms in the blow flies *Calliphora vicina* and *Lucilia richardsi* (Diptera: Calliphoridae)

Élise Camus[1,2], Ewan D. Finlayson[3], Pete Vukusic[3], Olivier Deparis[1], and Sébastien R. Mouchet[1,3,4,5,*]

[1] Department of Physics & Namur Institute of Structured Matter (NISM), University of Namur (UNamur), Rue de Bruxelles 61, 5000 Namur, Belgium
[2] Département de Physique, École Normale Supérieure de Lyon/Université Claude Bernard Lyon 1, 46 Allée d'Italie, 69364 Lyon Cedex 07, France
[3] Department of Physics and Astronomy, University of Exeter, Stocker Road, Exeter EX4 4QL, United Kingdom
[4] Institute of Life, Earth and Environment (ILEE), University of Namur (UNamur), Rue de Bruxelles 61, 5000 Namur, Belgium
[5] Micro- and Nanophotonic Materials Group & Research Institute for Materials Science and Engineering, University of Mons, Place du Parc 20, 7000 Mons, Belgium

Received 23 September 2025 / Accepted 3 December 2025

Abstract. Structural colours in natural organisms are created by complex photonic architectures giving rise to remarkable visual appearances. In arthropods, these structures are usually made of biopolymers and comprise photonic crystals. They are often iridescent, i.e., their colours depend on the incidence and observation angles. Despite the interest of the scientific community in a large variety of species including those belonging to butterflies and beetles, some orders such as dipterans have been overlooked so far. In this work, the structural colours from the abdomens of two dipteran species, namely *Calliphora vicina* and *Lucilia richardsi* blow flies, with different displayed colours were investigated by spectrophotometry and optical simulations. Using electron microscopy, we identified multilayer photonic structures as the primary mechanism responsible for their visual appearances, with possible additional thin-film interference in *C. vicina*. In addition, the dipterans' colours were analysed in terms of chromaticity as well as with respect to the visual sensitivities of the species and the ones of some of their predators. The reflectance spectra of the blow flies investigated were found to correlate with high absorption by their own and their predators' photoreceptors. These findings indicate that structural colouration in blow flies may influence not only communication with conspecifics but also interactions with predators.

Keywords: Structural colour, Natural photonic crystal, Photonic bandgap materials, Bragg mirror, Diptera, Blow fly.

1 Introduction

Structurally coloured living organisms exhibit complex optical structures leading to striking visual appearances [1–4]. In insects, these structures are often photonic crystals made of biopolymers such as chitin. A signature of the interference origin of such structural colours is iridescence, i.e., the displayed colours depend on the incidence and viewing angles. Many species have attracted much attention from the natural photonics scientific community since the 19th century such as butterfly species from the family Nymphalidae (e.g., *Morpho* genus), the family Papilionidae (e.g., *Papilio* genus) and the family Lycaenidae (e.g., *Polyommatus* genus) [1, 5] or beetle species from the family Buprestidae (e.g., *Chrysochroa* genus) and the family Scarabaeidae (e.g., *Chrysina* genus) [6]. However, species from some orders such as Diptera have been far from extensively investigated. In this work, we analysed the structural colours from the abdomens of different but related dipteran species from the family Calliphoridae, namely *Calliphora vicina* (Robineau-Desvoidy 1830, formerly known as *Calliphora erythrocephala*) and *Lucilia richardsi* (Collin 1926), each displaying various structural colours (Fig. 1). Most species in the order Diptera are known to exhibit colours from pigment origin. For instance, black visual appearances are associated with melanin [7]. Green colourations of adult specimens of some species from the family Chironomidae originate from bilin pigments [7]. These pigments are metabolic products of porphyrin compounds found in the haemoglobin at the origin of red colours in the larvae of the related species [7]. However, already in 1927, Mason described the colour of *Lucilia* sp. "and other "blue bottle" flies" as "metallic iridescent" due to a relatively thin colour-producing layer [8]. In 1935, Fraenkel described that the cuticle of newly

* Corresponding author: sebastien.mouchet@umons.ac.be

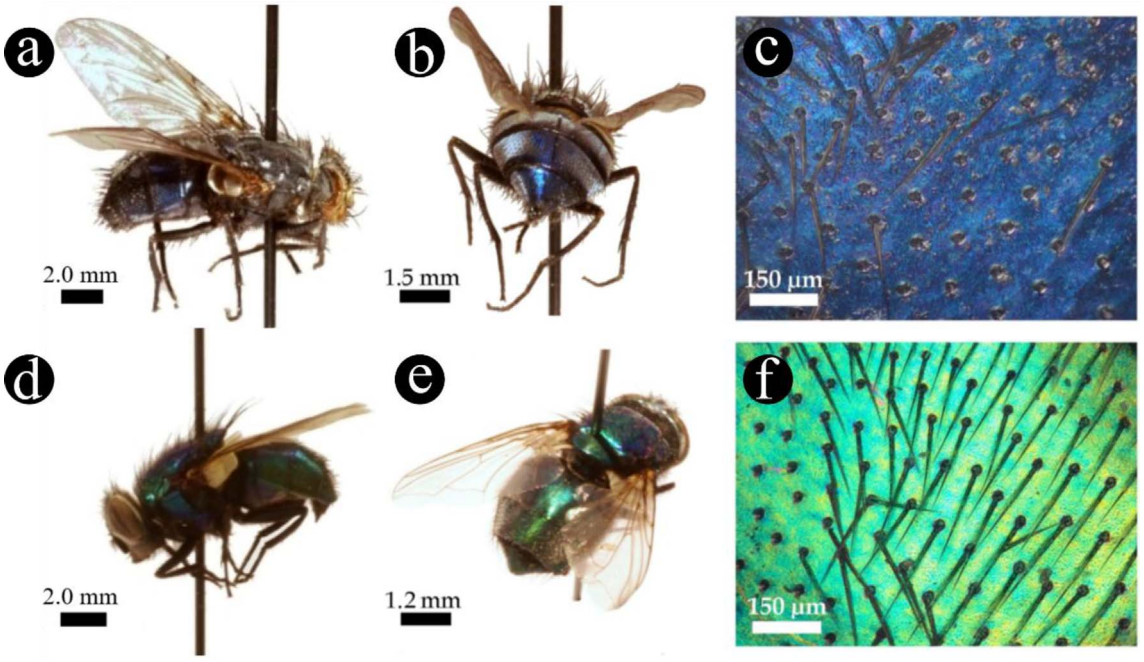

Figure 1. *Calliphora vicina* (a–c) and *Lucilia richardsi* (d–f) blow flies displays vivid iridescent blue and green colours, respectively, on their abdomens and thoraxes. Optical microscopy (c, f) allowed to observe black hairs (i.e., macrotrichia) with lengths ranging between ca. 200 and 300 µm (c, f).

emerged *C. vicina* blow flies turns from grey to blue about two hours after emergence [9]. Such a process can be inhibited in some circumstances [9, 10]. The interference origin of this species colouration was revealed by immersion in chloroform, leading to a colour change to green [10]. More recently, the colouration variations of iridescent *Lucilia sericata* blow fly were investigated as a function of temperature (from ambient temperature up to 220 °C) [11]. A periodic multilayer made of about 15 bilayers was observed in the cuticle of this insect. The bilayers were described by the superposition of a chitin layer the thickness of which was in the range 130–150 nm and a layer of air with a thickness ranging from 15 nm to 20 nm. Such multilayer epidermal structures in some species including wasps, flies, and beetles from the mid-Cretaceous have undergone a fossilisation process [12, 13]. In the case of an amber-entombed wasp species, Hou and coworkers demonstrated that the original structural colours were preserved through fossilisation. Unlike structural colours in dipteran cuticles, the optical properties of the eyes of many species (including *Chrysomyia megacephala*, *Musca domestica* and *C. vicina*) ranging from their colours to the sensitivities of their photoreceptors and autofluorescence were extensively investigated [14–24]. Blow flies such as *C. vicina* and *L. richardsi* have red eyes due to red-scattering screening pigments situated in their eyes' pigment cells [19]. In addition to dipteran eyes' optical properties, thin film interference was also found at the origin of the vivid iridescent colours of the wings of small Hymenoptera and Diptera [25, 26]. In *Drosophila spp.* and *Chrysomya spp.*, the wing patterns were demonstrated to play a role in sexual selection [26–28]. For instance, in the case of *Drosophila melanogaster*, males with more vivid magenta wings are more attractive to females [27]. Similarly, it was demonstrated that *Lispe cana* male flies actively orient their iridescent sexual displays on their faces and wings toward the sun under full sunlight to enhance sexual signal visibility [29].

C. vicina and *L. richardsi* blow flies are necrophagous species. The former has been widely investigated in forensic sciences [30–32]. The post-feeding larval dispersal is an important element in the estimation of the post-mortem interval of human cadavers. Later on, *L. richardsi* was demonstrated to have a similar interest for forensic investigation [33]. These flies are indeed attracted not only by decaying flesh [34] but also by faeces [35]. In addition, they are known to be disease and infection vectors [36]. Due to its significant flight agility, *C. vicina* attracted attention from the research field of biomechanics. The neuromuscular control of steering forces on this insect during flight were investigated [37]. Within the insect's cuticle, mechanoreceptors, called campaniform sensilla and with the shape of elliptical holes, deform under strain [38, 39]. Through a bioinspiration approach, strain sensors embedded in space structures were developed [39].

In this research, using electron microscopy, different multilayers were found to be the mechanisms for the colour appearances of both investigated species. Photonic multilayers are widespread among natural photonic structures. They occur in the cuticles and wings of structurally coloured species of Hymenoptera [40], Lepidoptera [5] and Coleoptera [6, 41–44]. In addition to spectral measurements and optical simulations, we analysed the dipterans' colours in terms of chromaticity as well as with respect to the visual sensitivities of the species and of some of their predators.

2 Materials and methods

In this study, we combined specimen collection and taxonomic identification with detailed morphological and optical analyses, as well as optical simulations. Structural features of the abdominal cuticle were examined by optical and electron microscopy, while spectral reflectance was measured to characterise the insects' optical responses. Chromaticity and photoreceptor quantum catch calculations were used to assess the visibility of the colours to conspecifics and predators. Finally, the observed structures were modelled to link physical structure to optical behaviour.

2.1 Specimen identification

Samples of *C. vicina* and *L. richardsi* were collected either naturally dead or alive in the province of Namur, Belgium and the city of Exeter, UK between 2013 and 2017. The specimens that were collected alive were chemically euthanized in a jar containing ethyl acetate. All samples were kept without any further conservation methods in room conditions of temperature and humidity. They were identified using identification keys [45–48].

2.2 Photonic structure morphology

Optical microscopy was performed using an Olympus BX61 (Tokyo, Japan) microscope, an Olympus XC50 camera and a halogen Osram HLX 64625 (Munich, Germany) visible white light source. The dipteran abdomens were observed in the reflection mode of the microscope. The abdomens of dead dipterans were dissected with a scalpel and placed on microscope slides covered by black paper. The flatter areas of the samples were observed.

The morphology of the dipteran abdomens' structures was investigated using a JEOL 7500F (Tokyo, Japan) field emission scanning electron microscope (SEM) and a JEOL JEM-1400 transmission electron microscope (TEM). For SEM analysis, abdomens were cut into pieces of about 5 mm × 5 mm. Some samples were immersed into liquid nitrogen immediately before being broken. This process increased the probability of a neat fracture. All SEM samples were attached to the sample mount by conducting double-sided adhesive tape and sputter-coated with 10 nm of gold. The dipteran abdomens were prepared following a standard TEM sample preparation method [49]. 80 nm-thick cross sections were ultramicrotomed and transferred onto TEM analysis grids. The layer thicknesses were measured along a line perpendicular to the multilayers, using image processing software ImageJ [50]. Measurements were taken at multiple positions in each selected micrograph. For *C. vicina*, 8 SEM images were analysed, while 5 TEM images were used for *L. richardsi*.

2.3 Optical characterisation

The normalised reflection spectra, also called reflection factor, $R(\lambda) = \{I(\lambda) - B(\lambda)\}/\{W(\lambda) - B(\lambda)\}$, i.e., the ratio between the spectral intensities $I(\lambda)$ and $W(\lambda)$ reflected by the sample and by an Ocean Optics WS-1 (Dunedin, Florida, USA) white reference, respectively, including noise corrections (namely, spectral intensity in darkness) $B(\lambda)$, were measured using an Avantes AvaSpect-2048 (Apeldoorn, The Netherlands) spectrophotometer, unpolarised visible light from an Ocean Optics DH-2000-BAL source and optical fibres in specular configuration (i.e., incidence and detection angles with the same magnitude). The analysed spot size extended over a few square millimetres. A fibre holder allowed measurements to be performed for angles ranging from −75° to 75° with respect to normal incidence, in steps of 15°.

From the reflection spectra, CIE 1931 coordinates (x, y, z) were calculated [51–53]. They allow the quantification of the colours perceived by the human eye and the two independent coordinates (x, y) are presented on a 2-degree observer chromaticity diagram. In these calculations, the spectrum of the incident light source was assumed to be the CIE standard illuminant D_{65}, corresponding to the average daylight emitted by the Sun (considered as a 6500 K black body) and received in Northern Europe.

Such a chromaticity diagram is however not valid for other species' colour perception. The spectral sensitivities of the photoreceptors located in eyes differ indeed from one species to another. In addition, some species have colour vision involving a different number of photoreceptors, such as some birds and some insects with tetrachromatic vision, i.e., four different types of photoreceptors, unlike human vision, which is trichromatic.

To gauge the visibility of the species to predators and conspecifics, the quantum catches of the photoreceptors associated with Calliphoridae species and three of their known predators, namely *Parus caeruleus* Eurasian blue tit, *Zootoca vivipara* common lizard and *Vespula vulgaris* common wasp, were calculated using the method suggested by Vorobyev et al. [54–56] These quantities correspond to the relative amount of photons absorbed by each type of photoreceptor related to a given species. In addition to the three kinds of photoreceptors, namely the short wavelength sensitive (SWS), the middle wavelength sensitive (MWS) and the long wavelength sensitive (LWS) cone photoreceptors, involved in the colour vision of these four selected species, the blow flies, the Eurasian blue tit, and the common lizard possess a fourth type of photoreceptors, namely very short wavelength sensitive (VSW) cone photoreceptors. The calculation of the related quantum catches requires the spectral sensitivities of these photoreceptors. This data was taken from the literature [19–21, 57–60].

2.4 Photonic model of the blow fly cuticle and numerical methods

A conventional one-dimensional transfer-matrix (1D-TM) method [61] was used to simulate the spectral reflectance from the structures observed in the dipteran integuments. This method rigorously solves Maxwell's equations in each layer of a photonic multilayer structure for both transverse electric (TE) and transverse magnetic (TM) polarisation of electromagnetic waves propagating through such layered media. In this formalism, the electromagnetic field wave is

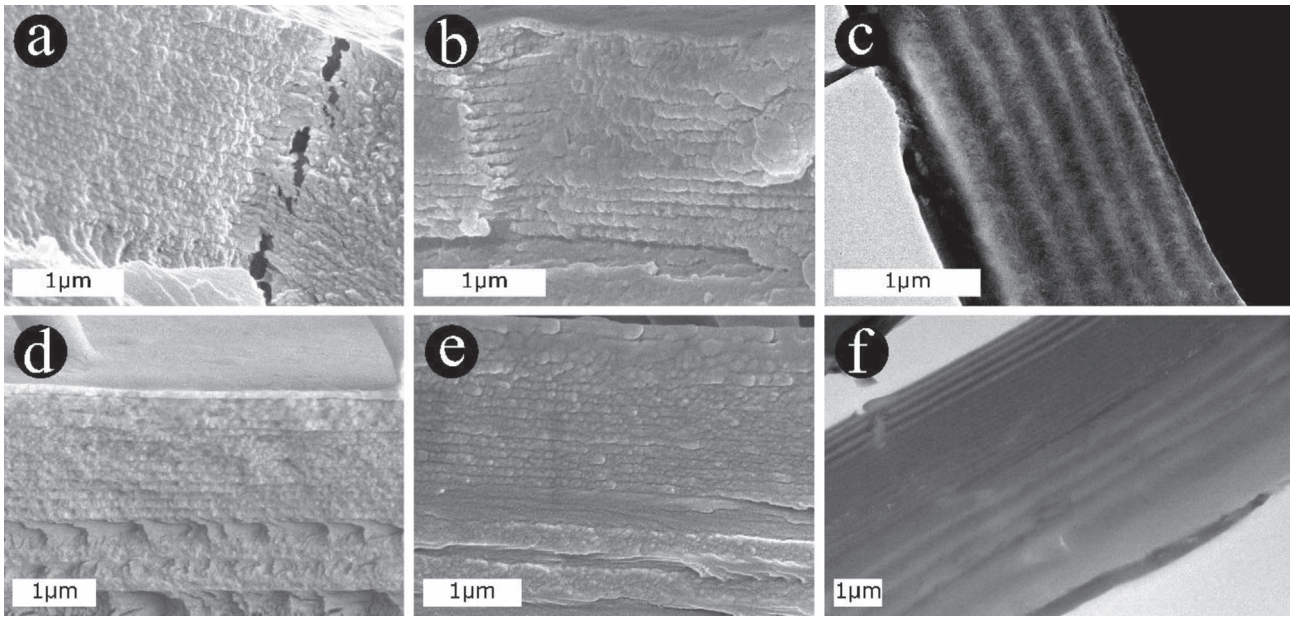

Figure 2. The photonic structures found in the cuticle of *Calliphora vicina* (a–c) and *Lucilia richardsi* (d–f) are multilayer reflectors, as observed by SEM (a, b, d, e) and TEM (c, f). One such single periodic multilayer is observed in *C. vicina*'s cuticle (a–c). It is made of two kinds of layer with thickness equal to 98 ± 7 nm and 20 ± 6 nm. *L. richardsi*'s cuticle comprises three multilayers: a top multilayer with 4 bilayers, the layers of which have a thickness equal to 78 ± 15 nm and 82 ± 12 nm; a middle multilayer containing about 25 layers, namely 13 58 ± 14 nm-thick dark contrasted layers and 12 60 ± 13 nm-thick light contrasted layers; and a bottom aperiodic multilayer composed of 3 light contrasted layers with thicknesses ranging from 175 nm to 370 nm and 3 dark contrasted layers.

decomposed in each layer into forward and backward waves propagating in the direction perpendicular to the layers.

The photonic band structures were calculated in the specific case of infinite one-dimensional photonic crystal based on the photonic structures observed in the dipteran cuticles using a Kronig–Penney model approach [62].

3 Results and discussion

Observations by optical microscopy revealed, in both cases, cuticles exhibiting quite homogeneous, shiny and metallic visual appearances (Figs. 1c, 1f). These cuticles are covered by black hairs, also called macrotrichia, the length of which ranges between ca. 200 and 300 µm. In addition, much shorter hairs, known as microtrichia, of about 20 µm can be observed by SEM (Fig. S1). Observations of cross-sections of the blow flies' cuticles by SEM and TEM showed the photonic structures inside their integuments (Fig. 2). In the case of *C. vicina*, one single periodic planar multilayer was observed by SEM (Figs. 2a, 2b). It comprises 18 periods with the appearance of two layers, the thicknesses of which were measured to be 98 ± 7 nm and 20 ± 6 nm (Figs. 2a, 2b). Both layers have different contrasts (dark and light contrasted, respectively) with SEM techniques. In the case of *L. richardsi*, three different multilayers are observed (Figs. 2d–2f). The top multilayer consists of 4 bilayers, the layers of which have thicknesses equal to 78 ± 15 nm and 82 ± 12 nm. The middle multilayer contains about 25 layers, namely 13 58 ± 14 nm-thick electron-dense layers and 12 60 ± 13 nm-thick electron-lucent layers. The bottom aperiodic multilayer is composed of 3 electron-lucent layers with thicknesses ranging from 175 nm to 370 nm and 3 electron-dense layers with thicknesses ranging from 120 nm to 160 nm. These structures contrast to some extent with the multilayer observed in the exocuticle of the green-coloured *L. sericata* blow fly, which exhibits about 15 periods comprising two layers described as being 130–150-nm and 15–20-nm thick layers [11].

Under incident light normal to the samples, the specular spectral reflectance from the blow flies' cuticles exhibits peaks located at 437 ± 8 nm and 537 ± 6 nm in the cases of *C. vicina* and *L. richardsi*, respectively (Fig. 3). These peaks were observed to blue-shift in combination with a decrease of their full width at half maximum (FWHM), when the incidence and detection angles increase (Figs. 3a, 3c, 4). Such a metallic iridescent optical response is typical of a multilayer reflector [61]. For a human perception point of view, this corresponds to colour changes following a curved path, from blue to violet and from green to violet, respectively, on the CIE chromaticity diagram (Figs. 3b, 3d).

Interestingly, TEM observations of the one-dimensional photonic structure in *C. vicina*'s cuticle showed patterns that might be associated with a Bouligand structure (Fig. 2c). Such structures were found in the cuticles of

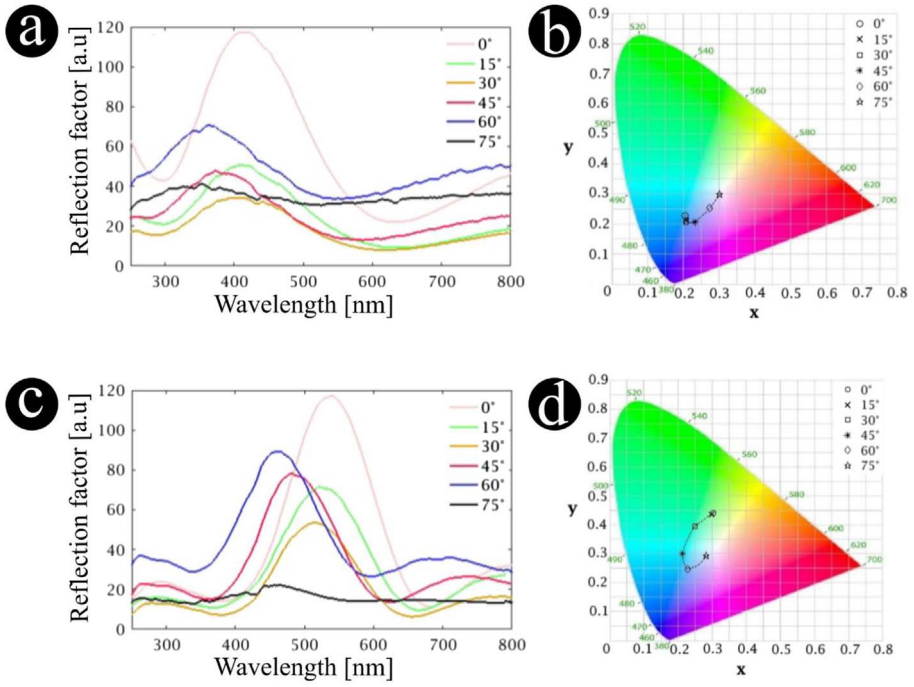

Figure 3. The specular spectral reflectance (quantified in terms of reflection factor) from *Calliphora vicina* blow fly peaks at 437 ± 8 nm at normal incidence (a), corresponding to a blue visual appearance, as observed on a chromaticity diagram (b). With increasing incidence and viewing angles, the reflectance peak blue-shifts (a) giving rise to violet colourations (b). In addition, a narrowing of the peak FWHM is observed. *Lucilia richardsi* blow fly's reflectance peak is located at 537 ± 6 nm at normal incidence (c), leading to a green colouration (d). With grazing incidence and observation angles, the reflectance peak narrows and blue-shifts (c) leading to blue and violet colours (d).

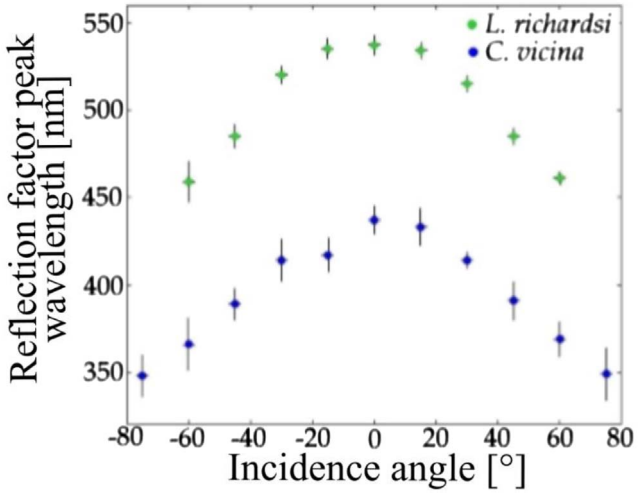

Figure 4. The spectral reflectance peaks measured from the abdomens of both *Calliphora vicina* and *Lucilia richardsi* (and quantified here in terms of reflection factor) blue-shift with increasing incidence and observation angles (in absolute values). Such a behaviour is typical of a multilayer reflector.

numerous species from the order Coleoptera and are known for their light circularly polarising properties [6, 63–68]. They consist of incrementally rotated birefringent layers stacked upon each other. Dipteran vision is known to be sensitive to light linear polarisation [15] and circular polarisation vision was demonstrated in other insects such as beetles [69], dragonflies [70], and damselflies [70], and more generally, in arthropods [71] including stomatopod crustaceans [72]. Polarised-light experimental techniques were used in order to measure circularly polarised (CP) reflectance components (further detail available in the electronic supplementary material). The possibility of the presence of a Bouligand structure may undermine the conclusion that the one-dimensional photonic structure is a non-chiral multilayer. Both co-CP and cross-CP configurations were hence investigated, where co-CP corresponds to incident and reflected CP components with the same handedness (left or right) and cross-CP refers to different handedness of the incident and reflected CP components. Despite this TEM observation, only cross-CP responses, similar to that of a planar mirror, displayed significant intensities (Fig. S2). The absence of the typical Bouligand structure's optical response might be explained by the small number of layers with respect to what was observed in other insects [6, 64–67]. Another likely explanation is that the birefringence contrast in refractive indices along the ordinary and extraordinary axes is not sufficiently high in order to give rise to co-CP reflection. A last possibility involving a thin film overlaying the Bouligand structure is discussed at the end of this section.

As mentioned above, the CIE chromaticity diagram is not valid for the colour perception of other animals. We therefore analysed the colour sensation from the

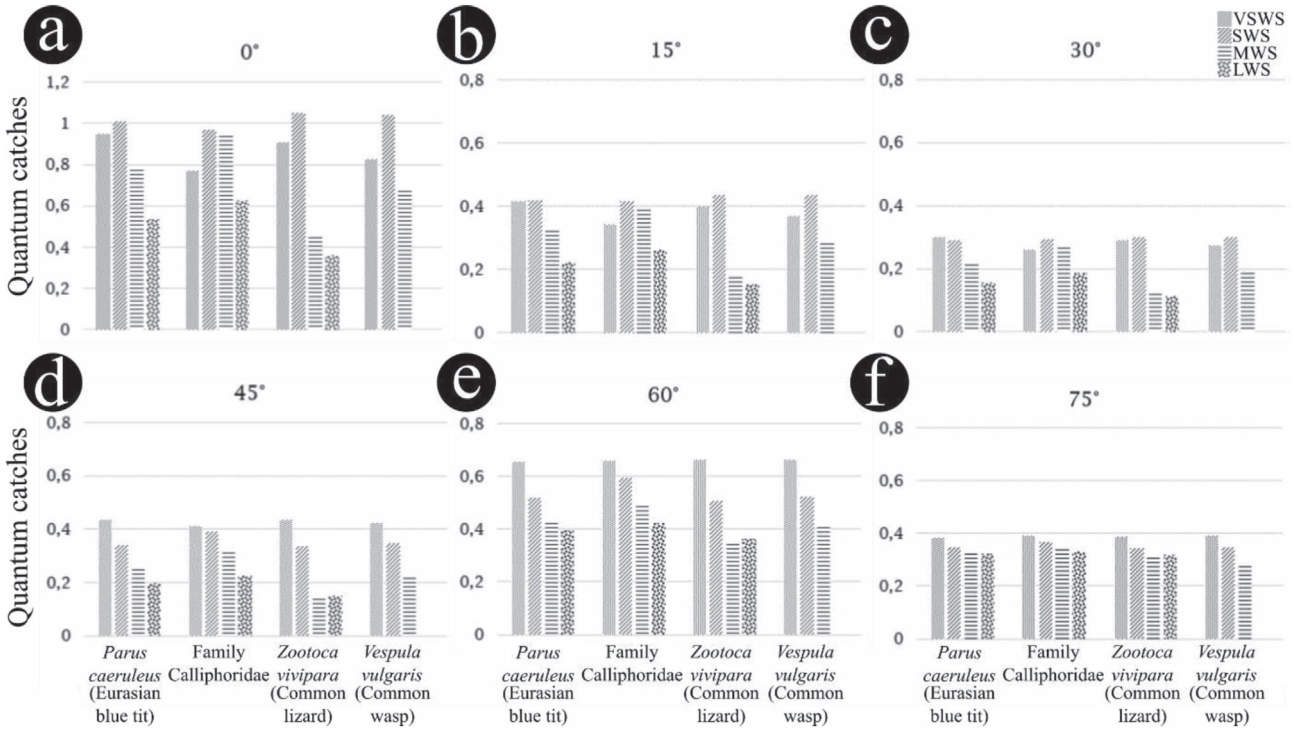

Figure 5. *Calliphora vicina*'s visual appearance is very intense for the visual systems of Calliphoridae species (blow flies), *Parus caeruleus* Eurasian blue tit, *Zootoca vivipara* lizard and *Vespula vulgaris* wasp, as shown here in terms of quantum catches. The reflectance peak located at 437 nm leads to high absorption by the SWS photoreceptors of all tetrachromatic vision species.

investigated blow flies' cuticles for different organisms including *C. vicina* (Fig. 5) and *L. richardsi* (Fig. 6) blow flies themselves as well as some of their predators (i.e., *P. caeruleus* Eurasian blue tit, *Z. vivipara* lizard and *V. vulgaris* wasp) by calculating the quantum catches related to their photoreceptors. From this analysis, we cannot directly infer the species colour perception since it would require to take into account the light transmission through the organisms' eye lenses and their neural processing of visual signals. In dipterans, for instance, visual sensitivity and colour discrimination vary widely among taxa and are often tuned to ecologically relevant cues such as host or mate detection [19–21, 57]. In addition, the visual background strongly affects detectability. In a specific background, a body colour that can be perceived may still remain undetected. For instance, camouflage strategies evolved in some species for millions of years involve mimetism through homomorphy and chromomorphy [73, 74]. Some observations can however be performed based on the calculated quantum catches. All selected species' visual systems are highly sensitive to *C. vicina* and *L. richardsi*'s visual appearances. *C. vicina*'s colour is specifically intense for all the four species. Its reflectance peak at normal incidence and detection (located at 437 nm) gives rise to a high absorption by the SWS photoreceptors of all four investigated species with both trichromatic and tetrachromatic visions. This colouration appears very chromatic in the case of the common lizard, i.e., the quantum catches among the photoreceptor types differ the most, resulting in a highly saturated colour signal. With larger incidence and detection angles, these four species' VSWS photoreceptors are more excited than their SWS photoreceptors. These organisms have a vision well suited for this blow fly's blue colour since they have types of photoreceptors in this range, namely SWS and VSWS. *L. richardsi*'s visual appearance at normal incidence and observation leads to a high absorption by the LWS photoreceptors of the Eurasian blue tit and the blow fly as well as by the MWS photoreceptors of the common lizard and the common wasp. This is due to its reflectance peak at 537 nm. If *L. richardsi* seems to be very chromatic for all four species, the common lizard is the species having the most chromatic sensation of this visual appearance. With higher incidence and detection angles, the photoreceptors absorbing the most reflected light also change: down to the SWS photoreceptors in the cases of the Eurasian blue tit, the common lizard and the common wasp and down to the MWS photoreceptors in the case of the blow fly.

The optical responses of the investigated blow flies' photonic structures were simulated as perfect photonic crystal models (Fig. 7) using the geometrical parameters measured from the electron microscopy observations (Fig. 2) in order to assess whether the measured reflectance spectra arise from the structures observed by SEM and TEM. In the case of *L. richardsi*, only the top multilayer was found to have dimensions that could be responsible for the optical behaviour of the cuticle. The thicknesses of the layers composing the bottom multilayer are too large for giving rise to an optical photonic bandgap in the range of interest. The middle multilayer could give rise to a predicted reflectance peak in the near UV range. However such a peak is not measured by spectrophotometry. This might be explained by a lack of refractive index contrast between both kinds of layer.

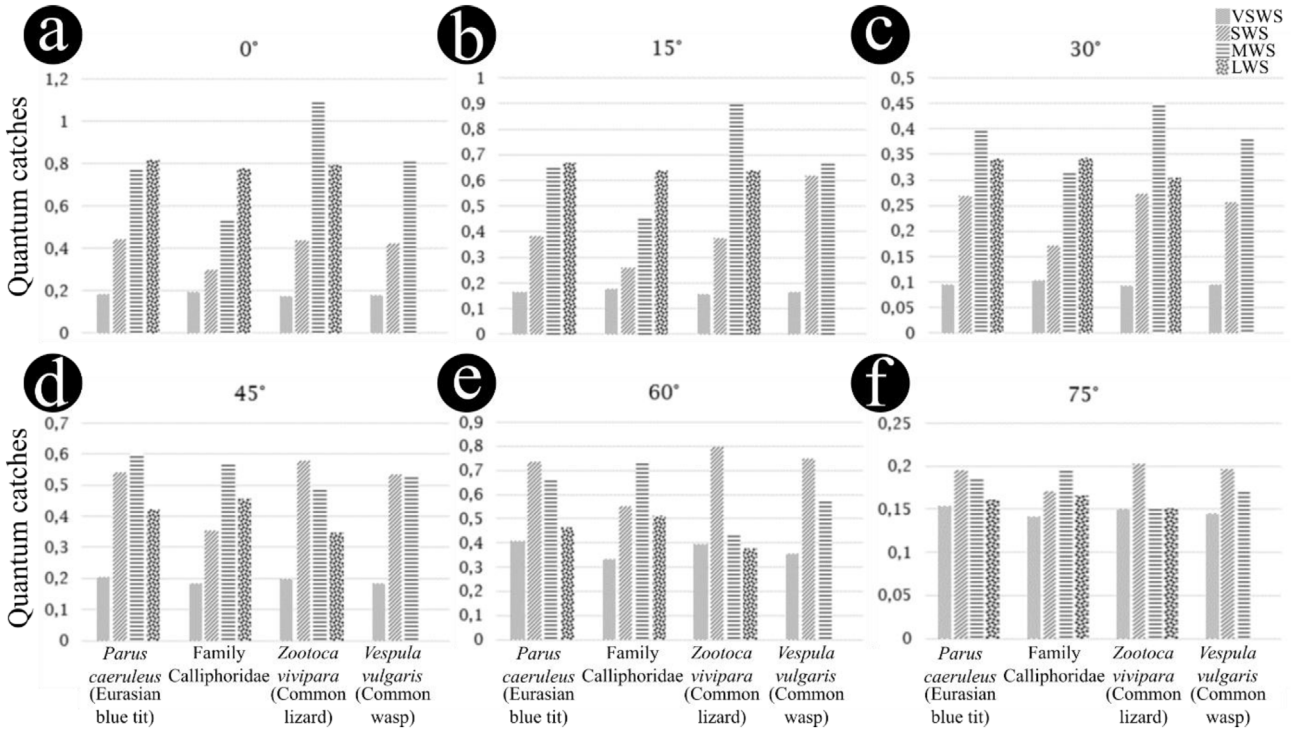

Figure 6. The visual systems of Calliphoridae species (blow flies), *Parus caeruleus* Eurasian blue tit, *Zootoca vivipara* lizard and *Vespula vulgaris* wasp are all highly sensitive to *Lucilia richardsi*'s visual appearance, as shown here in terms of quantum catches. Due to its reflectance peak at 537 nm, *L. richardsi*'s colour gives rise to a high absorption by the LWS photoreceptors of the Eurasian blue tit, the blow fly and the common wasp as well as by the MWS photoreceptors of the common lizard.

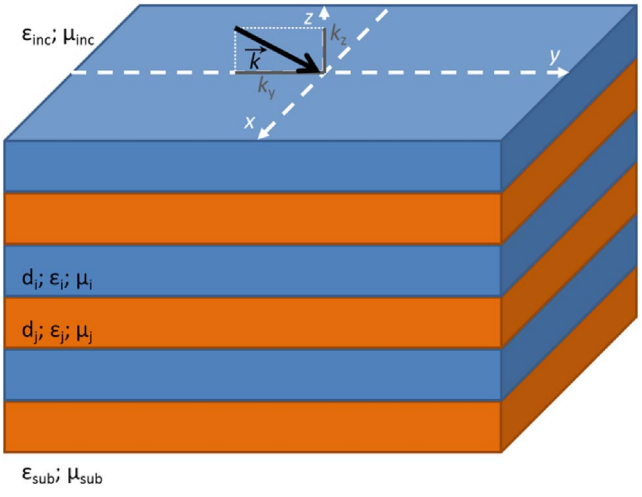

Figure 7. The photonic structures occurring in *Calliphora vicina* and *Lucilia richardsi*'s cuticle were modelled by multilayer periodic reflectors made of a stack of two different kinds of layers with thicknesses d_i and d_j, magnetic permeabilities $\mu_i = 1$ and $\mu_j = 1$ as well as dielectric permittivities $\varepsilon_i = 1.68^2$ and $\varepsilon_j = 1.55^2$ [75]. The incidence medium and the substrate have, respectively, magnetic permeabilities $\mu_{inc} = 1$ and $\mu_{sub} = 1$ as well as dielectric permittivities $\varepsilon_{inc} = 1.00^2$ and $\varepsilon_{sub} = 1.68^2$ [75]. Vector $\vec{k}$ represents incident wave vector.

Indeed, in TEM images, both kinds of layer are much less contrasted in the middle multilayer than in the top multilayer. The layers in the middle multilayer have therefore a more homogeneous electron opacity than in the top layer. The materials in these layers could be relatively similar, with a weak refractive index contrast. For *C. vicina*, the 98-nm and 20-nm layers were assigned refractive indices (RI) of 1.68 and 1.55, respectively; for *L. richardsi*, the 78-nm and 82-nm layers were assigned RI values of 1.68 and 1.55, respectively. These dispersionless values are good compromises between published values for butterfly scales and beetle cuticle [76–80] and correspond to the RI measured in the layers of *Chrysochroa rajah* beetle [80]. The RI of the incident medium and the substrate were taken equal to 1.00 and 1.68. The same structural models were used for both reflectance spectra and photonic band structures. However, for the calculation of the photonic band structures, the number of bilayers was assumed infinite. The simulated reflectance spectra and photonic band structures (Fig. 8) are in accordance with the experimental results. In the case of *C. vicina* and *L. richardsi*, the simulated reflectance peak and photonic bandgap (PBG) are located at 395 nm and at 517 nm at normal incidence, respectively. Both results are in accordance with the experimental results (experimental errors are smaller than 10%). Both the simulated reflectance peak and PBG blue-shift to 337 nm and to 436 nm at grazing incidence, for *C. vicina* and *L. richardsi*'s models, respectively. The predicted weak oscillations in the reflectance spectra are due to Fabry-Pérot interferences. They are related to the total multilayer thicknesses. They are not observed experimentally since the multilayer interface are not perfectly parallel in the actual dipteran cuticles and the multilayer

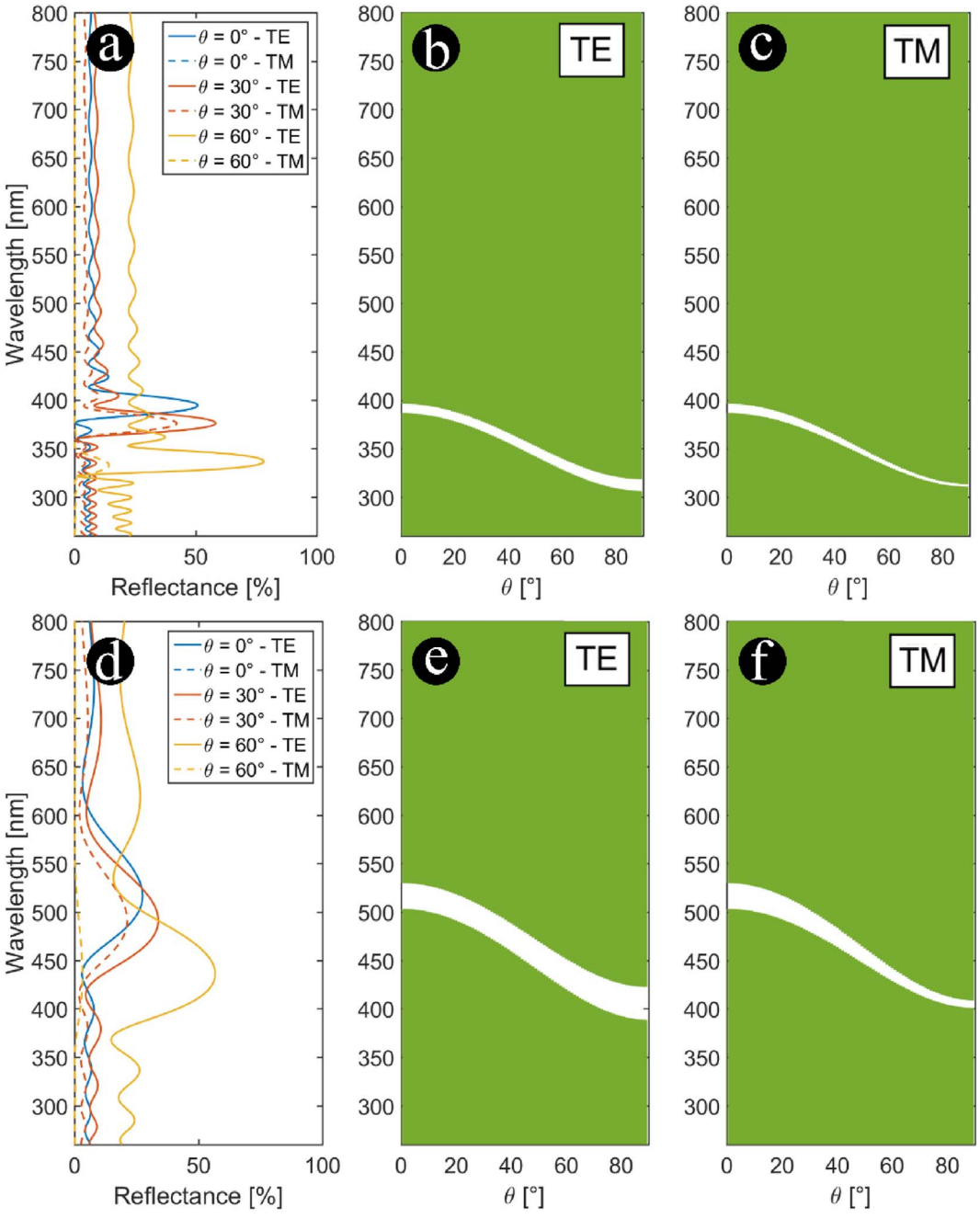

Figure 8. Reflectance spectra (a, d) and photonic band structures as a function of the incidence angle for TE (b, e) and TM (c, f) polarisations in the cases of the photonic models corresponding to *Calliphora vicina* (a–c) and *Lucilia richardsi*'s (d–f) photonic structures. Green areas correspond to allowed photonic bands.

thicknesses are much larger than the incident light coherence length.

The simulated optical responses of the multilayer models generally match the experimental reflectance spectra in both peak position and angular dependence. The accordance between experimental and numerical results demonstrates the photonic origin of the visual appearances of the investigated blow flies. For *C. vicina*, however, the simulated reflectance peak is noticeably narrower than the experimental one. This difference could arise from imperfections in the multilayer structure, such as random variations in layer thicknesses, and from the fact that experimental measurements were averaged over a relatively large solid angle. To assess this effect, we modelled a pseudo-periodic multilayer with random thickness deviations of ± 15 nm in the high-contrast layers and ± 5 nm in the low-contrast layers, and averaged the resulting calculated spectra over incidence angles from −5° to +5° (Fig. S3). This approach produced a broader peak than the ideal model, though still narrower than the measured spectrum.

An alternative explanation is thin-film interference in an additional ca. 180 nm-thick surface layer covering the epicuticle and the observed photonic structure. Such a layer could plausibly correspond to a wax and cement secretion deposited via pore canals after cuticle formation, as reported in insects [81, 82]. Simulations incorporating this layer yield a broad reflectance peak near 420 nm at normal incidence (Fig. S4a), in close agreement with the measured peak position. The presence of such a thin film could also explain the negligible intensities of detectable co-CP light reflection in the visible range if an underlying Bouligand structure with sufficient in-plane birefringence were present, since the thin-film interference can mask this signal (Fig. S4b). Furthermore, no such distinct superficial layer was observed in SEM or TEM images.

4 Conclusions

Unlike butterflies and beetles, the visual appearances of species from orders such as dipterans have not attracted much attention despite their striking colourful iridescence. In this work, the structural colours of *C. vicina* and *L. richardsi* blow flies' abdomens were investigated. The colourations displayed by *C. vicina* and *L. richardsi* are blue and green, respectively, with their reflectance spectra at normal incidence peaking at 437 ± 8 nm and 537 ± 6 nm. They are primarily due to photonic structures in the cuticles of these insects, as revealed by electron microscopy, consisting of one-dimensional periodic multilayers that produce metallic iridescence. In *C. vicina*, we cannot entirely exclude the possibility of thin-film interference from a superficial epicuticular layer over a likely Bouligand structure imaged by TEM. This interference could contribute to the observed reflectance properties and help explaining the negligible intensities detected in co-CP reflectance spectra. However, no such thin-film layer was directly observed in our SEM or TEM analyses. Both species appear bright and chromatic with respect to the visual sensitivities of blow flies and three selected predators. These sensations are mainly due to the high absorption by the SWS and VSWS photoreceptors, in the case of *C. vicina* and of the LWS, MWS and SWS photoreceptors, in the case of *L. richardsi*. These results suggest that structural colouration in blow flies may play roles beyond visual signalling to conspecifics, potentially influencing predator-prey dynamics.

Acknowledgments

The authors thank Serge Berthier (Institut des NanoSciences de Paris), Nicolas Reckinger (UNamur), Corry Charlier (UNamur) and Caroline De Bona (UNamur) for technical help during measurements. This research used resources of the "Plateforme Technologique de Calcul Intensif (PTCI)"[1] of UNamur, which is supported by the Belgian National Fund for Scientific Research (FRS-FNRS)-"Fonds de la Recherche Fondamentale Collective" (FRFC), the Walloon Region, and UNamur (Conventions No. 2.5020.11, GEQ U.G006.15, 1610468, RW/GEQ2016 and U.-G011.22). PTCI is a member of the "Consortium des Équipements de Calcul Intensif (CÉCI)"[2]. This research also used the resources of the Electron Microscopy Service (SME) of UNamur[3] and the Bioimaging Centre of the University of Exeter[4].

Funding

É Camus was supported by the ENS de Lyon and the Auvergne-Rhônes-Alpes region via an Explo'RA SUP scholarship as well as the European Union through the Erasmus+ program. SR Mouchet was supported by Wallonia-Brussels International (WBI) through a Postdoctoral Fellowship for Excellence program WBI.WORLD and by the Belgian National Fund for Scientific Research (FRS-FNRS) as a Postdoctoral Researcher and as an Associate Researcher. This research was also supported by FRS-FNRS through the Researchers' Credit CC 1.5075.11F.

Conflicts of interest

The authors declare have no competing interests.

Data availability statement

Data available from the Zenodo Repository: https://doi.org/10.5281/zenodo.17857389.

Author contribution statement

SRM conceived the original project. ÉC conducted the species identification, measured the reflectance spectra, calculated the CIE coordinates and the quantum catches, as well as performed the morphological characterisation by optical microscopy and SEM. SRM performed the TEM observations. EDF and SRM conducted the co- and cross-CP reflectance spectrophotometry. SRM, ÉC, and EDF performed the simulations. ÉC, EDF, PV, OD and SRM discussed the results. SRM wrote the manuscript with input from ÉC. All authors commented on the manuscript and gave approval to its final version.

Supplementary material

Supplementary material 1

Figure S1. Top view of the cuticle of *Calliphora vicina*'s abdomen using SEM. In addition to long hairs (known as macrotrichia) observed by optical microscopy, shorter hairs (also called microtrichia) of about 20 µm can be observed.

Supplementary material 2

Co- and cross-circularly polarised reflectance spectrophotometry.

The dipteran cuticles were characterised using cross- and co-circularly polarised (CP) reflectance spectrophotometry. Both co-CP and cross-CP configurations were investigated, where co-CP corresponds to incident and reflected CP components with the same handedness (left (L) or right (R)) and cross-CP refers to different handedness of the incident and reflected CP components. The experimental set-up, detailed in [65], consisted of an Ocean Optics (Delray Beach, FL, USA) USB2000+ spectrometer and an Ocean Optics HPX-2000 xenon broadband fibre-coupled light source. CP incident light beam was generated by a rotatable polariser and an achromatic Fresnel rhomb quarter-wave retarder, orientated at 45° azimuth. The CP light handedness was selected by orientating the polariser azimuth at either 0° or 90°.

[1] https://platforms.unamur.be/ptci.

[2] http://www.ceci-hpc.be.

[3] https://platforms.unamur.be/microscopie-electronique.

[4] http://biosciences.exeter.ac.uk/bioimaging/.

The incident light was focused onto a piece of Diptera cuticle at normal incidence using an achromatic × 10 objective lens, leading to a beam spot diameter of ca. 30 µm. This lens collected light backscattered by the sample, which was conducted by a beam-splitter through a CP analyser comprising the Fresnel rhomb and a second rotatable polariser. A plane aluminium mirror was used for the measurement calibration.

Supplementary material 3

Figure S2. CP reflectance spectrophotometry was used in order to highlight possible light-polarising effects arising from the pattern observed within *Calliphora vicina*'s cuticle that might be associated with a Bouligand structure. Despite the electron micrograph observations, only cross-CP components have significant intensities. Co-CP reflectance spectra that usually contains the signature of Bouligand structures display negligible intensities.

Supplementary material 4

Figure S3. Reflectance spectra of a pseudo-periodic multilayer derived from *Calliphora vicina* photonic model (Fig. 7) with random thickness deviations of ± 15 nm in the high-contrast layers and ± 5 nm in the low-contrast layers. The resulting calculated spectra were averaged over incidence angles from −5° to +5°. A broader reflectance peak than the ideal model (Fig. 8a) is observed, though still narrower than the measured spectrum (Fig. 3a).

Supplementary material 5

CP reflectance was modelled for various incidence angles using a one-dimensional 4 × 4 matrix method for anisotropic multilayers [83]. The model comprises a Bouligand structure overlaid by an interferential thin film. The Bouligand structure contained 18 half-pitches of 118 nm, had an average refractive index of 1.56 [78], and exhibited an in-plane birefringence of 0.018 [66]. The overlying thin film was modelled as a 180-nm thick isotropic layer with a refractive index of 1.75. All materials were assumed to be non-absorbing.

Supplementary material 6

Figure S4. For comparison, CP reflectance was modelled for a Bouligand structure (18 half-pitches of 118 nm, an average refractive index of 1.56 [78], in-plane birefringence of 0.018 [66]) covered by a 180 nm-thick isotropic film (n = 1.75), calculated for incidence and emergence angles ranging from 0° to 75° in 15° increments in cross-CP configuration (a) and at normal incidence in co- and cross-CP configuration (b). Modelled CP reflectance spectra in (a) appear as broad as the experimental spectra measure from *Calliphora vicina* (Fig. 3a). The left-left co-CP (LCP-LCP) spectrum exhibits a small peak in the UV range. In the real photonic structure of *C. vicina*, positional disorder [44], light absorption, and scattering would likely reduce this co-CP signal to a very weak level.

The supplementary material of this article is available at https://jeos.edpsciences.org/10.1051/jeos/2025053/olm.

References

1 Berthier S, La couleur des papillons ou l'impérative beauté - Propriétés optiques des ailes de papillons (Springer, Paris, 2000).
2 Berthier S, Iridescences, les couleurs physiques des insectes (Springer, Paris, 2003).
3 Kinoshita S, Structural Colors in the Realm of Nature (World Scientific Publishing Co, Singapore, 2008).
4 Mouchet SR, Deparis O, Natural Photonics and Bioinspiration (Artech House, London, 2021).
5 Mouchet SR, Vukusic P, Structural colours in lepidopteran scales, Adv. Insect Physiol. 54, 1–53 (2018). https://doi.org/10.1016/bs.aiip.2017.11.002.
6 Seago AE, Brady P, Vigneron JP, Schultz TD, Gold bugs and beyond: a review of iridescence and structural colour mechanisms in beetles (Coleoptera), J. R. Soc. Interface 6, S165–S184 (2009). https://doi.org/10.1098/rsif.2008.0354.focus.
7 Vukusic P, Chittka L, Visual signals: color and light production, in The Insects: Structure and Function, edited by R. F. Chapman, 5th edn. (Cambridge University Press, Cambridge, 2013), pp. 793–822. https://doi.org/10.1017/CBO9780511818202.026.
8 Mason CW, Structural colors in insects III, J. Phys. Chem. 31, 1856–1872 (1927). https://doi.org/10.1021/j150282a008.
9 Fraenkel G, Observations and experiments on the blow-fly (*Calliphora erythrocephala*) during the first day after emergence, P. Zool. Soc. Lond. 105, 893–904 (1935). https://doi.org/10.1111/j.1469-7998.1935.tb06269.x.
10 Wolfe S, Studies of the development of the imaginal cuticle of *Calliphora erythrocephala*, Q. J. Microsc. Sci. 95, 67–78 (1954). https://doi.org/10.1242/jcs.s3-95.29.67.
11 Martincek I, Pudis D, Satka A, Janigova I, Csomorova K, Cernobila F, Temperature effect on optical properties of the cuticle of *Lucilia sericata*, Optik 119, 523–527 (2008). https://doi.org/10.1016/j.ijleo.2007.02.009.
12 Cai C, Tihelka E, Pan Y, Yin Z, Jiang R, Xia F, Huang D, Structural colours in diverse Mesozoic insects, Proc. R. Soc. B 287, 20200301 (2020). https://doi.org/10.1098/rspb.2020.0301.
13 Hou Z, Cai D, Dong R, Structural color in Amber-entombed wasp: A detailed study using NS-FDTD simulations, IEEE Access 12, 57163–57171 (2024). https://doi.org/10.1109/ACCESS.2024.3389505.
14 Beersma DGM, Stavenga DG, Kuiper JW, Organization of Visual Axes In The Compound Eye Of The Fly *Musca domestica* L. and behavioural consequences, J. Comp. Physiol. 102, 305–320 (1975). https://doi.org/10.1007/BF01464343.
15 McCann GD, Arnett DW, Spectral and polarization sensitivity of the dipteran visual system, J. Gen. Physiol. 59, 534–558 (1972). https://doi.org/10.1085/jgp.59.5.534.
16 Tinbergen J, Stavenga DG, Photoreceptor redox state monitored *in vivo* by transmission and fluorescence microspectrophotometry in blowfly compound eyes, Vision Res. 26, 239–243, (1986). https://doi.org/10.1016/0042-6989(86)90018-0.
17 Smits RP, Jansonius NM, Stavenga DG, Dependence of receptor potential and redox state of mitochondrial cytochromes on oxygen fraction measured in the blowfly eye *in vivo*, J. Comp. Physiol. A 177, 105–110 (1995). https://doi.org/10.1007/BF00243402.
18 Stavenga DG, Tinbergen J, Light dependence of oxidative metabolism in fly compound eyes studied in vivo by microspectrofluorometry, Naturwissenschaften 70, 618–620 (1983). https://doi.org/10.1007/BF00377410.
19 Stavenga DG, Colour in the eyes of insects, J. Comp. Physiol. A 188, 337–348 (2002). https://doi.org/10.1007/s00359-002-0307-9.
20 Stavenga DG, Angular and spectral sensitivity of fly photoreceptors. III. Dependence on the pupil mechanism in the blowfly *Calliphora*, J. Comp. Physiol. A 190, 115–129 (2004). https://doi.org/10.1007/s00359-003-0477-0.

21 Stavenga DG, Surface colors of insects: wings and eyes, in Functional Surfaces in Biology, edited by S.N. Gorb, 1st edn. (Springer, Dordrecht, 2009), pp. 285–306. https://doi.org/10.1007/978-1-4020-6697-9_15.

22 Stavenga DG, Meglič A, Pirih P, Koshitaka H, Arikawa K, Wehling MF, Belušič G, Photoreceptor spectral tuning by colorful, multilayered facet lenses in long-legged fly eyes (Dolichopodidae), J. Comp. Physiol. A 203, 23–33 (2017). https://doi.org/10.1007/s00359-016-1131-y.

23 Stavenga DG, Wehling MF, Belušič G, Functional interplay of visual, sensitizing and screening pigments in the eyes of *Drosophila* and other red-eyed dipteran flies, J. Physiol. 595, 5481–5494 (2017). https://doi.org/10.1113/JP273674.

24 van Hateren JH, Hardie RC, Rudolph A, Laughlin SB, Stavenga DG, The bright zone, a specialized dorsal eye region in the male blowfly *Chrysomyia megacephala*, J. Comp. Physiol. A 164, 297–308 (1989). https://doi.org/10.1007/BF00612990.

25 Shevtsova E, Hansson C, Janzen DH, Kjærandsen J, Stable structural color patterns displayed on transparent insect wings, P. Natl Acad. Sci. USA 108, 668–673 (2011). https://doi.org/10.1073/pnas.1017393108.

26 Butterworth NJ, White TE, Byrne PG, Wallman JF, Love at first flight: wing interference patterns are species-specific and sexually dimorphic in blowflies (Diptera: Calliphoridae), J. Evol. Biol. 34(3), 558–570 (2021). https://doi.org/10.1111/jeb.13759.

27 Katayama N, Abbott JK, Kjærandsen J, Takahashi Y, Svensson EI, Sexual selection on wing interference patterns in *Drosophila melanogaster*, P. Natl Acad. Sci. USA 111, 15144–15148 (2014). https://doi.org/10.1073/pnas.1407595111.

28 Hawkes MF, Duffy E, Joag R, Skeats A, Radwan J, Wedell N, Sharma MD, Hosken DJ, Troscianko J, Sexual selection drives the evolution of male wing interference patterns, Proc. R. Soc. B 286, 20182850 (2019). https://doi.org/10.1098/rspb.2018.2850.

29 White TE, Latty T, Flies improve the salience of iridescent sexual signals by orienting toward the sun, Behav. Ecol. 31(6), 1401–1409 (2020). https://doi.org/10.1093/beheco/araa098.

30 Arnott S, Turner, B, Post-feeding larval behaviour in the blowfly, *Calliphora vicina*: Effects on post-mortem interval estimates, Forensic Sci. Int. 177, 162–167 (2008). https://doi.org/10.1016/j.forsciint.2007.12.002.

31 Gomes L, Godoy WAC, Von Zuben CJ, A review of postfeeding larval dispersal in blowflies: implications for forensic entomology, Naturwissenschaften 93, 207–215 (2006). https://doi.org/10.1007/s00114-006-0082-5.

32 Striman B, Fujikawa A, Barksdale L, Carter DO, Alteration of expirated bloodstain patterns by *Calliphora vicina* and *Lucilia sericata* (Diptera: Calliphoridae) through ingestion and deposition of artifacts, J. Forensic Sci. 56, S123–S127 (2011). https://doi.org/10.1111/j.1556-4029.2010.01575.x.

33 Szpila K, Hall MJR, Pape T, Grzywacz A, Morphology and identification of first instars of the European and Mediterranean blowflies of forensic importance. Part II. Luciliinae, Med. Vet. Entomol. 27, 349–366 (2013). https://doi.org/10.1111/j.1365-2915.2012.01059.x.

34 Kuusela S, Hanski I, The structure of carrion fly communities: the size and the type of carrion, Holarct. Ecol. 5, 337–348 (1982). https://doi.org/10.1111/j.1600-0587.1982.tb01048.x.

35 Blackith RE, Blackith RM, Differential attraction of calyptrate flies (Diptera) to faeces, J. Nat. Hist. 27, 645–655 (1993). https://doi.org/10.1080/00222939300770371.

36 Stevens J, Wall R, The Evolution of Ectoparasitism in the Genus *Lucilia* (Diptera: Calliphoridae), Int. J. Parasitol. 27, 51–59 (1997). https://doi.org/10.1016/S0020-7519(96)00155-5.

37 Balint CN, Dickinson MH, Neuromuscular control of aerodynamic forces and moments in the blowfly, *Calliphora vicina*, J. Exp. Biol. 207, 3813–3838 (2007). https://doi.org/10.1242/jeb.01229.

38 Gnatzy W, Grünert U, Bender M, Campaniform sensilla of *Calliphora vicina* (Insecta, Diptera), Zoomorphology 106, 312–319 (1987). https://doi.org/10.1007/BF00312005.

39 Vincent JFV, Clift SE, Menon C, Biomimetics of campaniform sensilla: Measuring strain from the deformation of holes, J. Bionic Eng. 4, 63–76 (2007). https://doi.org/10.1016/S1672-6529(07)60015-8.

40 Kroiss J, Strohm E, Vandenbem C, Vigneron JP, An epicuticular multilayer reflector generates the iridescent coloration in chrysidid wasps (Hymenoptera, Chrysididae), Naturwissenschaften 96, 983–986 (2009). https://doi.org/10.1007/s00114-009-0553-6.

41 Stavenga DG, Wilts BD, Leertouwer HL, Hariyama T, Polarized iridescence of the multilayered elytra of the Japanese jewel beetle, *Chrysochroa fulgidissima*, Phil. Trans. R. Soc. B 366, 709–723 (2011). https://doi.org/10.1098/rstb.2010.0197.

42 Pasteels JM, Deparis O, Mouchet SR, Windsor DM, Billen J, Structural and physical evidence for an endocuticular gold reflector in the tortoise beetle, *Charidotella ambita*, Arthropod Struct. Dev. 45, 509–518 (2016). https://doi.org/10.1016/j.asd.2016.10.008.

43 Mouchet SR, Lobet M, Kolaric B, Kaczmarek AM, Van Deun R, Vukusic P, Deparis O, Van Hooijdonk E, Photonic scales of *Hoplia coerulea* beetle: any colour you like, Mater. Today Proc. 4, 4979–4986 (2017). https://doi.org/10.1016/j.matpr.2017.04.104.

44 Mouchet SR, Luke S, McDonald LT, Vukusic P, Optical costs and benefits of disorder in biological photonic crystals, Faraday Discuss. 223, 9–48 (2020). https://doi.org/10.1039/D0FD00101E.

45 Rognes K, Revision of the Norwegian material of the genus *Dasyphora* Robineau-Desvoidy (Diptera, Muscidae) with new records of species and localities. Fauna norv. Ser. B 26, 49–58 (1979).

46 Stevens J, Wall R, Classification of the genus *Lucilia* (Diptera: Calliphoridae): a preliminary parsimony analysis, J. Nat. Hist. 30, 1087–1094 (1996). https://doi.org/10.1080/00222939600770581.

47 Mihályi F. A New Key for Hungarian Lucilia Species (Diptera, Calliphoridae), Ann. Hist.-Nat. Mus. Nat. Hung. 69, 181–184 (1977).

48 Szpila K, Key for identification of European and Mediterranean blowflies (Diptera, Calliphoridae) of forensic importance. Adult flies, Nicolaus Copernicus University, 1–18, 2010.

49 Vukusic P, Sambles JR, Lawrence CR, Wootton RJ, Quantified interference and diffraction in single *Morpho* butterfly scales. Proc. R. Soc. Lond. B 266, 1403–1411 (1999). https://doi.org/10.1098/rspb.1999.0794.

50 Schneider CA, Rasband WS, Eliceiri KW, NIH Image to ImageJ: 25 years of image analysis, Nat. Methods 9, 671–675 (2012). https://doi.org/10.1038/nmeth.2089.

51 Chamberlin GJ, Chamberlin DG, Colour: Its measurement, computation and application. (Heyden international topics in science, London, 1980).
52 Deparis O, Vandenbem C, Rassart M, Welch VL, Vigneron JP, Color-selecting reflectors inspired from biological periodic multilayer structures. Opt. Express 14, 3547–3555 (2006). https://doi.org/10.1364/OE.14.003547.
53 Judd DB, Wyszecki G, Color in business, science and industry. (John Wiley & Sons, New York, 1975).
54 Vorobyev M, Osorio D, Receptor noise as a determinant of colour thresholds. Proc. R. Soc. Lond. B 265, 351–358 (1998). https://doi.org/10.1098/rspb.1998.0302.
55 Vorobyev M, Marshall J, Osorio D, Hempel de Ibarra N, Menzel R, Colorful objects through animal eyes, Color Res. Appl. 26, S214–S217 (2001). https://doi.org/10.1002/1520-6378(2001)26:1+<::AID-COL45>3.0.CO;2-A.
56 Vorobyev M, Brandt R, Peitsch D, Laughlin SB, Menzel R, Colour thresholds and receptor noise: behaviour and physiology compared, Vision Res. 41, 639–653 (2001). https://doi.org/10.1016/S0042-6989(00)00288-1.
57 Lunau K, Visual ecology of flies with particular reference to colour vision and colour preference, J. Comp. Physiol. A 200, 497–512 (2014). https://doi.org/10.1007/s00359-014-0895-1.
58 Martin M, Le Galliard JF, Meylan S, Loew ER, The importance of ultraviolet and near-infrared sensitivity for visual discrimination in two species of lacerlid lizards, J. Exp. Biol. 218, 458–465 (2015). https://doi.org/10.1242/jeb.115923.
59 Ödeen A, Håstad O, Alström P, Evolution of ultraviolet vision in the largest avian radiation – the passerines, BMC Evol. Biol. 11, 313 (2011). https://doi.org/10.1186/1471-2148-11-313.
60 Peitsh D, Fietz A, Hertel H, de Souza J, Ventura DF, Menzel R, The spectral input systems of hymenopteran insects and their receptor-based colour vision, J. Comp. Physiol. A 170, 23–40 (1992). https://doi.org/10.1007/BF00190398.
61 Yeh P, Optical Waves in Layered Media. (Wiley-Interscience, Hoboken, 2005).
62 Vandenbem C, Contribution à l'étude de la réflectance et du confinement des modes dans les systèmes optiques stratifiés. Ph.D. thesis – Facultés Universitaires Notre-Dame de la Paix (FUNDP), Namur, 2006.
63 Bouligand Y, Sur l'existence de "Pseudomorphoses cholestériques" chez divers organismes vivants. J. Phys. Colloques 30, C4-90–C4-103 (1969). https://doi.org/10.1051/jphyscol:1969424.
64 Fernández del Río L, Arwin H, Järrendahl K, Polarizing properties and structure of the cuticle of scarab beetles from the *Chrysina genus*, Phys. Rev. E 94, 012409 (2016). https://doi.org/10.1103/PhysRevE.94.012409.
65 Finlayson ED, McDonald LT, Vukusic P, Optically ambidextrous circularly polarized reflection from the chiral cuticle of the scarab beetle *Chrysina resplendens*, J. R. Soc. Interface 14, 20170129 (2017). https://doi.org/10.1098/rsif.2017.0129.
66 McDonald LT, Finlayson ED, Wilts BD, Vukusic P, Circularly polarized reflection from the scarab beetle *Chalcothea smaragdina*: light scattering by a dual photonic structure, Interface Focus 7, 20160129 (2017). https://doi.org/10.1098/rsfs.2016.0129.
67 Mendoza-Galván A, Fernández del Río L, Järrendahl K, Arwin H, Graded pitch profile for the helicoidal broadband reflector and left-handed circularly polarizing cuticle of the scarab beetle *Chrysina chrysargyrea*. Sci. Rep. 8, 6456 (2018). https://doi.org/10.1038/s41598-018-24761-w.
68 Neville AC, Levy S, The helicoidal concept in plant cell wall ultrastructure and morphogenesis, in Biochemistry of Plant Cell Walls, edited by C.T. Brett, J.R. Hilman (Cambridge University Press, Cambridge, 1985), pp. 99–124.
69 Warrant EJ, Polarisation Vision: Beetles see circularly polarised light, Curr. Biol. 20(14), R610–R612 (2010). https://doi.org/10.1016/j.cub.2010.05.036.
70 Roucourt Cezário R, Marques Lopez V, Datto-Liberato F, Bybee SM, Gorb S, Guillermo-Ferreira R, Polarized vision in the eyes of the most effective predators: dragonflies and damselflies (Odonata), Sci. Nat. 112(1), 8 (2025). https://doi.org/10.1007/s00114-025-01959-3.
71 Homberg U, el Jundi B, Polarization Vision in Arthropods, edited by J.S. Werner, L.M. Chalupa (MIT press, Cambridge, 2013), pp. 1207–1217.
72 Chiou TH, Kleinlogel S, Cronin T, Caldwell R, Loeffler B, Siddiqi A, Goldizen A, Marshall J, Circular polarization vision in a stomatopod crustacean, Curr. Biol. 18(6), 429–434 (2008). https://doi.org/10.1016/j.cub.2008.02.066.
73 Yamamoto N, Sota T, Evolutionary fine-tuning of background-matching camouflage among geographical populations in the sandy beach tiger beetle, Proc. Roy. Soc. B 287 (1941), 20202315 (2020). https://doi.org/10.1098/rspb.2020.2315.
74 Mark CJ, O'Hanlon JC, Holwell GI, Camouflage in lichen moths: Field predation experiments and avian vision modelling demonstrate the importance of wing pattern elements and background for survival, J. Anim. Ecol. 91(12), 2358–2369 (2022). https://doi.org/10.1111/1365-2656.13817.
75 Noyes JA, Vukusic P, Experimental method for reliably establishing the refractive index of buprestid beetle exocuticle, Opt. Express 15(7), 4351–4358 (2007). https://doi.org/10.1364/OE.15.004351.
76 Berthier S, Charron E, Da Silva A, Determination of the cuticle index of the scales of the iridescent butterfly *Morpho menelaus*. Opt. Commun. 228, 349–356 (2003). https://doi.org/10.1016/j.optcom.2003.10.032.
77 Caveney S, Cuticle reflectivity and optical activity in scarab beetles: the role of uric acid, Proc. R. Soc. Lond. B 178, 205–225 (1971). https://doi.org/10.1098/rspb.1971.0062.
78 Leertouwer HL, Wilts BD, Stavenga DG, Refractive index and dispersion of butterfly chitin and bird keratin measured by polarizing interference microscopy, Opt. Express 19, 24061–24066 (2011). https://doi.org/10.1364/OE.19.024061.
79 Sollas IBJ, On the Identification of Chitin by Its Physical Constants. Proc. R. Soc. Lond. B 79, 474–484 (1907). https://doi.org/10.1098/rspb.1907.0042.
80 Yoshioka S, Kinoshita S, Direct determination of the refractive index of natural multilayer systems, Phys. Rev. E 83, 051917 (2011). https://doi.org/10.1103/PhysRevE.83.051917.
81 Lenau T, Barfoed M, Colours and metallic sheen in beetle shells–A biomimetic search for material structuring principles causing light interference, Adv. Eng. Mater. 10(4), 299–314 (2008). https://doi.org/10.1002/adem.200700346.
82 Arwin H, Berlind T, Jobs B, Järrendahl K, Cuticle structure of the scarab beetle *Cetonia aurata* analyzed by regression analysis of Mueller-matrix ellipsometric data, Opt. Express 21(19), 22645–22656 (2013). https://doi.org/10.1364/OE.21.022645.
83 Ko DYK, Sambles JR, Scattering matrix method for propagation in stratified media: attenuated total reflection studies of liquid crystals, J. Opt. Soc. Am. A 5, 1863–1866 (1988). https://doi.org/10.1364/JOSAA.5.001863.